


The Na⁺/Ca²⁺ exchanger NCX3 mediates Ca²⁺ entry into matrix vesicles to facilitate initial steps of mineralization in osteoblasts

Irshad A. Sheikh¹ | Monica T. Midura-Kiela¹ | André Herchuelz² | Sophie Sokolow³ | Pawel R. Kiela^{1,4}  | Fayez K. Ghishan¹

¹Daniel Cracchiolo Institute for Pediatric Autoimmune Disease Research, Steele Children's Research Center, Department of Pediatrics, University of Arizona, Tucson, Arizona, USA

²Laboratoire de Pharmacodynamie et de Thérapeutique, Faculté de Médecine, Université Libre de Bruxelles, Bruxelles, Belgium

³School of Nursing, University of California, Los Angeles (UCLA), Los Angeles, California, USA

⁴Department of Immunobiology, University of Arizona, Tucson, Arizona, USA

Correspondence

Pawel R. Kiela, and Fayez K. Ghishan, Department of Pediatrics, University of Arizona, 1501 N. Campbell Ave., Tucson, AZ 85724, USA.
Email: pkiela@arizona.edu and fghishan@peds.arizona.edu

Abstract

Matrix vesicles (MVs) provide the initial site for amorphous hydroxyapatite (HA) formation within mineralizing osteoblasts. Although Na⁺/Ca²⁺ exchanger isoform-3 (NCX3, SLC8A3) was presumed to function as major Ca²⁺ transporter responsible for Ca²⁺ extrusion out of osteoblast into the calcifying bone matrix, its presence and functional role in MVs have not been investigated. In this study, we investigated the involvement of NCX3 in MV-mediated mineralization process and its impact on bone formation. Using differentiated MC3T3-E1 cells, we demonstrated that NCX3 knock-out in these cells resulted in a significant reduction of Ca²⁺ deposition due to reduced Ca²⁺ entry within the MVs, leading to impaired mineralization. Consequently, the capacity of MVs to promote extracellular HA formation was diminished. Moreover, primary osteoblast isolated from NCX3 deficient mice (NCX3^{-/-}) exhibits reduced mineralization efficacy without any effect on osteoclast activity. To validate this in vitro finding, μ CT analysis revealed a substantial decrease in trabecular bone mineral density in both genders of NCX3^{-/-} mice, thus supporting the critical role of NCX3 in facilitating Ca²⁺ uptake into the MVs to initiate osteoblast-mediated mineralization. NCX3 expression was also found to be the target of downregulation by inflammatory mediators in vitro and in vivo. This newfound understanding of NCX3's functional role in MVs opens new avenues for therapeutic interventions aimed at enhancing bone mineralization and treating mineralization-related disorders.

KEYWORDS

matrix vesicles, mineralization, NCX3, osteoblasts

1 | INTRODUCTION

During skeletal development, remodelling and repair, osteoblasts (OB) initiate a highly complex physiochemical and biochemical process of mineralization. This process consists of two distinct phases: matrix vesicle-mediated mineralization, which refers to initial formation of mineral precursors and crystallization of hydroxyapatite (HA) crystals, followed by the subsequent collagen mineralization, that is, deposition of early HA crystals within collagen fibrils (Hasegawa, 2018, Kirsch et al., 1997). Matrix vesicles (MVs) are spherical electron-dense microparticles 100–300 nm in diameter which are believed to participate in all forms of physiological or ectopic calcification including bone, teeth, and cartilage. The initial synthesis of the amorphous calcium phosphate occurs within the confines of the intracellular MVs, which can transport inorganic phosphate (Pi) and Ca²⁺ from extracellular fluid (and perhaps the cytoplasm) into the MV lumen. Although the cellular biogenesis of MVs is still controversial, upon budding off the plasma membrane, MVs attach to collagen fibres, where the HA crystals, now more insoluble, accumulate sufficiently to

This is an open access article under the terms of the [Creative Commons Attribution-NonCommercial-NoDerivs License](https://creativecommons.org/licenses/by-nc-nd/4.0/), which permits use and distribution in any medium, provided the original work is properly cited, the use is non-commercial and no modifications or adaptations are made.

© 2024 The Author(s). *Journal of Extracellular Vesicles* published by Wiley Periodicals LLC on behalf of International Society for Extracellular Vesicles.

penetrate through the MV membrane, ultimately destroying the MVs, and becoming the foci of nucleation and further crystalline HA growth (Anderson et al., 2005; Bottini et al., 2018; Golub, 2009; Kirsch et al., 1994; Wuthier & Lipscomb, 2011). In addition to carrying mineralization-initiating enzymes such as tissue non-specific alkaline phosphatase (TNAP) and noncollagenous matrix proteins, MV are enriched with various cargo proteins (e.g., TNFRSF11B, WNT5A, SEMA4D) and microRNAs (miRNAs) such as miR-122-5p, miR-142-3p, miR-223-3p, and miR-451-5p which are known regulators of osteoclast and osteoblast development and participate in intercellular communication and signalling (Ansari et al., 2021; D'Angelo et al., 2001; Leach et al., 1995; Nahar et al., 2008; Wang et al., 2022; Wei et al., 2019). As an example, miR-125b accumulates in bone matrix where it inhibits osteoclastogenesis and bone resorption via downregulation of the transcriptional repressor PRDM1 (PR domain zinc finger protein 1). (Minamizaki et al., 2020) While the detailed characteristics and MV cargo remains an active research field, relatively little is known about its impact on bone remodelling.

One of the MV-related knowledge gaps is our understanding of the associated vesicular mineral transport process. Phosphoethanolamine/Phosphocholine Phosphatase 1 (PHOSPHO1) generates Pi from phosphocholine (PCho) and phosphoethanolamine (PE) within the MVs. Additionally, Pi can also be sourced from coupled function of two enzymes, Ectonucleotide Pyrophosphatase/Phosphodiesterase 1 (ENPP1) and biomineralization associated alkaline phosphatase (ALPL/TNAP), present on the outer membrane of MVs. ENPP1 uses adenosine triphosphate (ATP) to generate inorganic pyrophosphate (PPi), an inhibitor of mineralization, while TNAP promotes mineralization by converting PPi into Pi, creating a favourable microenvironment rich in Pi for the initiation of mineralization within MVs. This extravesicular Pi may be sensed and transported into the MVs by the Na⁺/Pi cotransporters, PiT-1 and PiT-2 (Pi Transporters 1 and 2; Hasegawa et al., 2022), although this remains to be experimentally verified. The process of Ca²⁺ delivery to the MVs to facilitate the formation of nascent HA within the vesicle lumen is even less clear. Current model assumes annexins, especially the abundant annexin A5 (ANXA5, annexin V) to form Ca²⁺ channels and mediate Ca²⁺ influx into MV (Kirsch, 2005; Rojas et al., 1992). However, investigating large unilamellar vesicles (LUV) as a model to study de novo mineralization within MV lumen revealed that ANXA5 only weakly supported ⁴⁵Ca²⁺ flux LUVs (Blandford et al., 2003). Moreover, Brachvogel et al. (Belluoccio et al., 2010) reported that double knockout of ANXA5 and ANXA6 in mice had no discernible effect on mineralization and skeleton development in vivo. These findings questioned the prevailing role of annexins as the primary Ca²⁺ channel required for MV-mediated mineralization and left a significant gap in our understanding the principal mechanism of Ca²⁺ entry into MV to initiate the primary mineralization.

In a proteomic analysis of murine OB-derived MVs, Xiao et al. (Xiao et al., 2007) identified a peptide signature of a Na⁺/Ca²⁺ exchanger consistent with Na⁺/Ca²⁺ exchanger NCX3, encoded by the SLC8A3 gene, thus creating a potential alternative pathway for Ca²⁺ transport in MVs. NCX3 has been shown to be expressed in mineralizing osteoblasts to contribute to Ca²⁺ translocation out of osteoblasts into calcifying bone matrix (Sosnoski & Gay, 2008; Stains et al., 2002), but its expression and role specifically in MVs has not been demonstrated thus far. The goal of this current study was to examine the expression and potential functional role of NCX3 in mediating Ca²⁺ entry into MVs to facilitate the synthesis of the amorphous HA during initial MVs mediated mineralization process of bone formation. Using a combination of genetic inactivation of *Slc8a3* in mice, human and mouse primary OBs and non-transformed mineralizing OB cell line (MC3T3-E1; mouse calvaria 3T3 cells, subclone E1), we define the role of NCX3 in regulating bone formation in vivo, expression pattern of NCX3 during mineralization, we provide evidence of NCX3 expression and importance for Ca²⁺ transport in MV and the reduced ability of NCX3-deficient MV to promote mineralization in a cell-free system. We also demonstrate that NCX3 is a target of inhibition by chronic inflammation and the associated inflammatory mediators.

2 | MATERIALS AND METHODS

2.1 | Mice

Frozen sperm of NCX3^{-/-} mice was generously provided by Dr. André Herchuelz (Sokolow et al., 2004). In vitro fertilization and establishment of a viable colony was performed by the University of Arizona Genetically Engineered Mouse Modeling (GEMM) core facility. Mice were tailed-tipped and genotyped by polymerase chain reaction (PCR) using the following primers: NCX3_F: CAGATAAGCGACTGCTCTTC, NCX3_R: CCTGGCTTCAGAACCACAGTG, and Neo: TCGACTAGAGGATCAGCTT at the final concentrations of 5 μM each, using MyTaq DNA polymerase (Bioline). Chronic colitis was induced in WT C56BL/6J mice in three cycles of 2.5% of dextran sodium sulphate (DSS) in the drinking given for 7 days, with 14-day recovery period in between. Mice were monitored daily for the symptoms of colitis, such as body weight loss, lethargy, loss of grooming and diarrhoea. At the conclusion of the study, colonic histology and mucosal mRNA expression of key inflammatory mediators [TNF (tumor necrosis factor), IFNγ (interferon gamma), IL1β (interleukin beta)] was analyzed to confirm disease development. All mice were housed in the specific pathogen-free animal barrier facility at the University of Arizona BIO5institute. Sentinel mice were routinely monitored and determined as free from common murine pathogens (mouse hepatitis virus, mouse parvovirus, minute virus of mice, Theiler's murine encephalomyelitis virus, Mycoplasma pulmonis, Sendai, epizootic diarrhoea of infant mice, murine

norovirus and ecto- and endoparasites). All animal protocols and procedures were approved by the University of Arizona Animal Care and Use Committee (protocol #07-126).

2.2 | Alizarin red/Alcian blue staining of the skeleton

The protocol for staining full term mouse skeleton was followed as described previously by McLeod with minor modification (McLeod, 1980). Following sacrifice, WT and NCX3^{-/-} mice were eviscerated and their skin was removed. The specimens were then fixed in 95% ethanol for 24 h and subsequently stained overnight in an Alcian blue solution (containing 150 mg Alcian blue, 800 mL 98% ethanol and 200 mL acetic acid). After several hours of rinsing with 95% ethanol, the samples were immersed in 2% KOH for 24 h, followed by additional staining in Alizarin red solution (50 mg/L Alizarin red in 2% KOH) for another 24 h. The skeletal specimens were preserved in a solution of 1% KOH and 20% glycerol until their skeletons became clearly visible, and then they were stored in a solution of 50% ethanol and 50% glycerol.

2.3 | Cell culture

A mineralizing subclone 4 of MC3T3-E1 osteoblast progenitor cell line was obtained from the American Type Culture Collection (ATCC number CRL-2593) and cultured in ascorbic acid (AA)-free α -MEM (minimal essential medium) growth media containing 10% foetal bovine serum (FBS; Hyclone), and 1% penicillin/streptomycin at 37°C with 5% CO₂. Under standard growth and maintenance conditions, the medium was replaced every 2 days and cells subcultured at 1:4 ratio with 0.25% trypsin at 80%–90% confluency. To induce osteogenic differentiation, confluent cultures were switched from growth media to osteogenic media, that is, complete α -MEM with exosome depleted FBS, 50 μ g/mL AA and 3 mM P_i and cultured for additional 21 days.

2.4 | Osteoclast isolation and differentiation

Primary osteoclasts from WT and NCX3^{-/-} mice were obtained following previously described protocol with minor modifications (Dai et al., 2018). Briefly, bone marrow from mouse femurs was flushed with α -MEM and centrifuged. Following erythrocyte depletion using a hypotonic buffer, the cells were cultured in α -MEM supplemented with 10% FBS for a period of 24 h. The non-adherent cells were then seeded in 100-mm uncoated dishes at a density of 5×10^6 cells per dish and cultured in the presence of M-CSF (30 ng/mL) for 3 days. The medium was then changed to α -MEM medium with 20 ng/mL M-CSF and 20 ng/mL RANKL for induction of osteoclast differentiation. After 5–6 days of culture, osteoclasts were stained using a leukocyte acid phosphatase kit (Sigma Aldrich, St. Louis, MO, USA). To determine TRAP activity, cells were fixed with 10% formalin for 10 min and followed by 95% ethanol for 1 min. Subsequently, 100 μ L of citrate buffer (50 mM, pH 4.6) with 10 mM sodium tartrate and 5 mM p-nitrophenylphosphate (Sigma-Aldrich) was added to the cells and incubated for 1 h. Enzymatic reactions were then transferred to new plates, mixed with an equal volume of 0.1 N NaOH and absorbance was measured at 410 nm using a microplate reader.

2.5 | Human primary osteoblasts

Primary human osteoblasts (HOB) were procured from PromoCell (cat. # C-12720) and cultured according to instructions provided by the vendor. Briefly, 3×10^4 HOB were seeded per well in a 24-well tissue culture plate and cultured in Osteoblast Growth Medium (PromoCell #C-27001) until confluency. Subsequently, the Osteoblast Growth Medium was replaced with Osteoblast Mineralization Medium (PromoCell #C-27020) and maintained for a duration of 21 days to induce mineralization.

2.6 | Generation of stable NCX3 knockout (KO) MC3T3-E1 cell lines

The Clustered Regularly Interspaced Short Palindromic Repeats (CRISPR) and CRISPR-associated protein (Cas9) system was used to ablate *Slc8a3* gene in MC3T3-E1 cells by using NCX3 Double Nickase Plasmid (sc-431066-NIC, Santa Cruz Biotechnology). Briefly, MC3T3-E1 cells were seeded at a density of 3×10^5 cells/well on a 6-well plate in antibiotic-free complete α -MEM growth media. Cells grown to 80% confluency transfected with 2.0 μ g of NCX3 Double Nickase Plasmid in transfection media. A plasmid containing a unique, non-targeting 20 nt scramble guide RNA (gRNA; sc-437281) was used as a negative control. Forty-eight hours post-transfection, green fluorescent protein (GFP)-positive cells were sorted using FACSAria III cell sorter with FACSDiva software (BD Biosciences), and the successfully transfected MC3T3-E1 cells grown in complete α -MEM growth media in the presence of 2.5 μ g/mL puromycin. Clonal selection was performed by serial dilution in a 96-well plate and two

stable NCX3^{-/-} MC3T3-E1 lines were selected for experiments after screening by western blot to confirm the absence of NCX3 protein. Some experiments were conducted with both clones with identical results; thus, the remainder of the work was done with clone #5 and only these results are presented here for clarity.

2.7 | Cell treatment and western blotting

WT and NCX3^{-/-} MC3T3-E1 cells were grown to confluence in 100-mm tissue culture dishes. For some experiments, cells were maintained in osteogenic media for 21 days post-confluence with proinflammatory cytokines (IFN γ (100U/mL), IL1 β (10 ng/mL) and TNF α (10 ng/mL) applied in the last 72 h. This approach was chosen to avoid the negative effects of early cytokine exposure on osteoblast differentiation (Gilbert et al., 2000) which would dramatically affect the yields of MVs and make the results difficult to compare and interpret. The 72-h period was as more representative of chronic inflammation and allowed for adequate accumulation of MVs in the media that permitted their isolation and downstream assays (24 h period was not sufficient).

Cells were washed with phosphate buffered saline (PBS) and homogenized by sonication in radioimmune precipitation assay (RIPA) buffer with protease inhibitor cocktail (1:100; Sigma, P8340). Protein concentration in the resulting cell lysates was determined using BCA Protein Assay (ThermoFisher Scientific) and samples were denatured in Laemmli sample buffer at 95°C for 5 min. After 10% SDS-PAGE (sodium dodecyl-sulfate polyacrylamide gel electrophoresis) separation and transfer to nitrocellulose, membranes were blocked with Tris-buffered saline with Tween-20 (TBST) containing 5% non-fat milk for 1 h and incubated with specific primary antibodies at 4°C overnight: NCX3 (1:1000, Alomone labs, ANX-013), TNAP (1:1000, R&D, AF2910-SP), Osteocalcin (1:1000, Takara, M188), β -actin (1:5000, Sigma, A5316), Pit-1 (1:1000, Invitrogen, PA5-28182). We used HRP-conjugated secondary antibodies and ECL (enhanced chemiluminescence) Western Blotting Substrate (Thermo Scientific) for chemiluminescent detection using the Syngene G:BOX Imaging System and GeneSys software.

2.8 | Real time RT-PCR analysis

Five hundred nanogram of total RNA harvested from cells isolated with TRIzol reagent were reverse transcribed into cDNA using the SensiFAST cDNA Synthesis Kit, (Bioline, cat # BIO-65054). Quantitative real-time PCR (qRT-PCR) was performed in 10 μ L reactions using Bioline mastermix (cat # BIO-86005) and FAM-conjugated primer/probe mixes for relevant targets (Applied Biosystems) using LightCycler96 thermocycler (Roche). Ct values were obtained using LightCycler96 software (version 1.1.0.1320) and were analyzed by the comparative cycle threshold (Ct) method as means of relative quantitation of gene expression, normalized to an endogenous reference (TATA-box binding protein [TBP]) and relative to a calibrator (normalized Ct value obtained from a respective control group), and expressed as 2^{- $\Delta\Delta$} Ct (Applied Biosystems User Bulletin number 2: Rev B “Relative Quantitation of Gene Expression”).

2.9 | Micro-CT evaluation and static histomorphometry

Eight- and 24-week old males and females C57BL/6 and NCX3^{-/-} mice were sacrificed and excised femurs were stripped of muscles and fixed with 10% formalin for 3 days and then kept in 70% ethanol until scanned by using a SkyScan 1172 micro-CT instrument at the New York University micro CT Core Lab. Bone mineral density (BMD), bone volume (BV/TV), trabecular spacing (Tb.Sp), trabecular number (Tb.N) and trabecular thickness (Tb.Th) were analyzed with the CT Analyzer program (Bruker micro-CT). For histomorphometric analysis, undecalcified bone samples were dehydrated, defatted and embedded in a clear methacrylate polymer plastic. After curing into hardened blocks, the bones were thin sectioned using a Leica RM2265 fully motorized rotary microtome into 16–20 five-micrometre-thick sections for each specimen. Masson's trichrome stain was used for the collection of data regarding bone volume as well as trabecular thickness, number and spacing. After staining, sections were imaged using either a Leica DMR/XE Universal or Leica-Aperio GL ScanScope microscope station, and digital images loaded into Bioquant Osteo Measure for image analysis and quantification purposes. All data acquisition was averaged from three sections per mouse.

2.10 | MVs isolation and nanoparticle tracking analysis (NTA)

Osteogenic media from MC3T3-E1 cells and primary calvaria cells were collected on Day 21 and MVs were harvested by ultracentrifugation as previously described (Johnson et al., 1999; Xiao et al., 2007). Briefly, osteogenic media were first cleared of cells and cellular debris by centrifugation at 20,000 \times g at 4°C for 30 min. To pellet the MVs, the supernatants were further centrifuged at 100,000 \times g at 4°C for 60 min (Optima LE-80K, fixed-angle rotor 45Ti, Beckman Coulter GmbH, Krefeld, Germany). In some

cases, microvesicles pellets were suspended in lysis buffer (1% Triton X-100 in 0.2 M Tris base with 1.6 mM MgCl₂, pH 8.1). Protein lysate was clarified by centrifugation at 13,000 × g for 15 min at 4°C and was stored at 20°C for later experiments. The size and concentration of the isolated matrix vesicles were analyzed using a NanoSight LM10-HS10 system instrument and equipped with scientific CMOS camera and 638 nm laser (NanoSight Amesbury, UK). Each matrix vesicles sample was diluted in 1 mL DPBS (Dulbecco's Phosphate Buffered Saline) to obtain a measurable concentration. A monochromatic laser beam in combination with NanoSight tracking software version 2.3 was used to analyze the size, size distribution profile and concentration of matrix vesicles.

2.11 | Cell-free MV-collagen calcification assay

Calcification mediated by isolated MVs was assessed in a cell-free assay as previously described (Chen et al., 2008, 2010). Briefly, glass coverslips were coated with type I collagen (0.01% in 0.1 M acetic acid) at room temperature for 4 h. MVs harvested from MC3T3-E1 or NCX3^{-/-} cells grown for 21 days in osteogenic conditions and 25 μg MV protein was added to type I collagen precoated glass coverslips and incubated with osteogenic media (MEMα with 15% FBS and 10 mM β-glycerophosphate). After 72 h incubation, the media is removed from the coverslips and decalcified with 0.6 N HCl for 24 h followed by colorimetric Ca²⁺ assay with *o*-cresolphthalein complexone method (Connerty & Briggs, 1966).

2.12 | Alizarin red staining

MC3T3-E1 cells and primary osteoblasts were seeded in six wells plates and cultured in osteogenic conditions for 21 days. Cells were washed with 1 × PBS twice and fixed with 4% paraformaldehyde at room temperature for 30 min. Next cells were washed three times with PBS and stained 2% Alizarin red S (pH 4.2) (Sigma) for 15 min at room temperature. The stained cells were photographed.

2.13 | Electron microscopy

Samples were fixed in 3% paraformaldehyde/0.5% glutaraldehyde in 0.1 M Pipes [piperazine-N,N'-bis(2-ethanesulfonic acid)] buffer pH 7.4 for 60 min at room temperature, washed in 0.1 M Glycine/PIPES buffer for 20 min, PIPES buffer for 10 min, deionized water (DIW) for 5 min, dehydrated through ethanol series to 90% and infiltrated with 50/50 London Resin (LR) White resin/90% ethanol overnight followed by LR White for 3 × 60 min. Samples were embedded in LR White in 00 gelatine capsules for 24 h at 50°C and 80 nm sections cut onto uncoated nickel grids using a Reichert UCT ultramicrotome. Sections were labelled with a 1:5 dilution of primary antibody against NCX3 in 0.1 M phosphate buffer overnight at 4°C and washed for 5 × 5 min in buffer. Secondary goat anti-rabbit antibody labelled with 10 nm gold was applied at 1:5 dilution overnight at 4°C. Sections without primary antibody were used as controls. Sections were counterstained with 2% lead citrate for 2 mins, washed with deionized water and viewed in a T12 electron microscope at 100 kV. Eight-bit TIFF images were collected using an AMT side-mount camera.

2.14 | Energy dispersive spectroscopy (EDS) analysis

The EDS analyses were performed in collaboration with the Kuiper Materials Imaging and Characterization Facility at University of Arizona. A 10 μL suspension of MVs made in sterile Dulbecco's PBS was deposited on lacey carbon-coated 300 mesh copper grids (SPI Supplies). The samples were air dried for 30 min at room temperature and observed under 200 kV HF5000 transmission electron microscope (TEM, Hitachi) equipped with an adapter for X-ray microanalysis Energy Dispersive Spectrometer (EDS, Oxford Instruments). The images and EDS mapping were taken in scanning transmission electron microscopy (STEM) mode. Three different types of images were generated simultaneously under STEM mode: dark field (DF), secondary electron (SE) and bright field (BF). The spectral and compositional analysis was performed, and the obtained data were expressed as a percentage of all of the sum of the known elements in the periodic table to indicate the content of Ca and P (as atomic %). The ratio of Ca/P for each sample was calculated.

2.15 | Statistical analysis

All the data in the bar graphs are expressed as mean ± SD. A value of $p < 0.05$ (versus the indicated group) was considered to indicate a statistically significant difference by one-way analysis of variance or Student's *t*-test (GraphPad Prism 7.0).

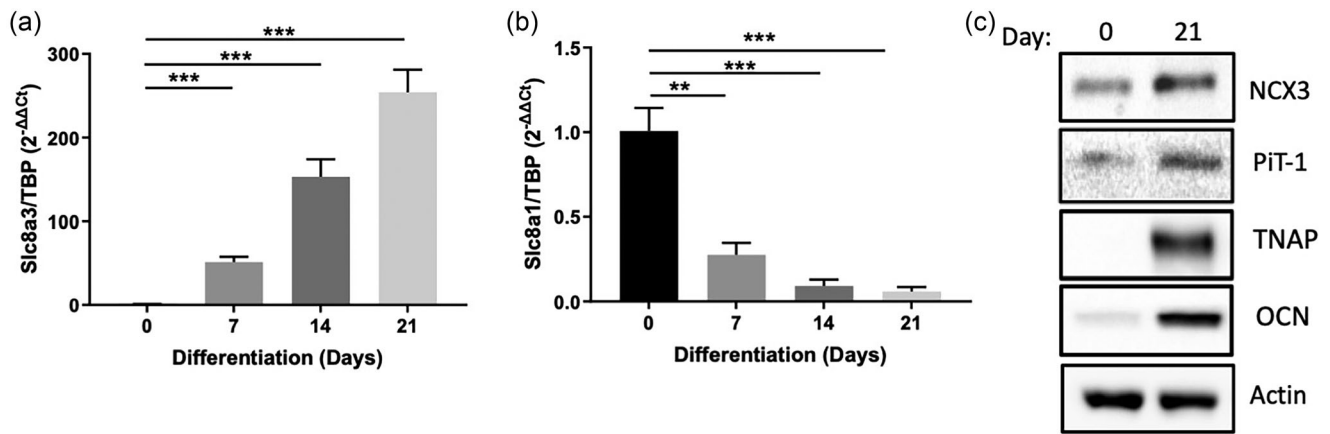


FIGURE 1 Osteoblast NCX3 mRNA expression increases during osteogenic differentiation. (a) qRT-PCR analysis of NCX3/*Slc8a3* and (b) NCX1/*Slc8a1* mRNA expression in MC3T3-E1 pre-osteoblasts during 21-day differentiation in osteogenic media. TATA-box Binding Protein (TBP) mRNA was used as an internal control ($n = 3$). Statistical significance was assessed using two-tailed Student's unpaired t -tests. Data are presented as the mean \pm SD (** $p < 0.01$, *** $p < 0.001$). (c) Western blotting analysis of total NCX3 and PiT-1 proteins during MC3T3-E1 pre-osteoblast differentiation. TNAP and OCN were used mineralization markers and β -actin was used as a loading control (representative of $n = 3$). NCX3, Na⁺/Ca²⁺ exchanger isoform-3; qRT-PCR, quantitative real-time PCR; TNAP, tissue non-specific alkaline phosphatase; OCN, osteocalcin.

3 | RESULTS

3.1 | NCX3 is necessary for osteoblast mineralization in vitro and bone density in vivo

Previous studies revealed that NCX3 is the predominant NCX isoform expressed by mineralizing osteoblasts, and its expression pattern and spatial distribution supported its role as a major contributor of Ca²⁺ translocation out of mineralizing osteoblasts into calcifying bone matrix (Sosnoski & Gay, 2008; Stains et al., 2002). In further support of these findings, we investigated the expression pattern of two major NCX isoforms, NCX1 and NCX3, in MC3T3-E1 preosteoblasts during differentiation under osteogenic conditions. We observed a progressive increase in NCX3 mRNA corresponding with an equally dynamic decline of NCX1 transcript during 21 days of osteogenic culture (Figure 1a,b). Immunoblotting also showed a significant increase in NCX3, as well as PiT-1 protein expression during 21 days of osteogenic differentiation in primary wild-type (WT) murine osteoblasts isolated (Figure 1c). Based on these observations and previously reported study, we set out to examine potential involvement of NCX3 in osteoblast-mediated mineralization.

NCX3^{-/-} mice did not demonstrate overt differences from their wild-type (WT) littermates in terms of breeding, body weight or gross skeletal abnormalities (Figure S1). To ascertain the in vivo impact of NCX3 deletion on bone metabolism, we performed μ CT analysis of femoral bones in 8-week-old male and female WT and NCX3^{-/-} mice. Trabecular bone parameter analysis showed significant deficits in bone formation in both sexes of NCX3^{-/-} mice, except for trabecular thickness, which was significantly reduced in males only (Figure 2a). Those differences persisted in 24-week-old mice (Figure S2). Cortical bone mineral density (BMD) tended to be lower in both male and female NCX3^{-/-} mice ($p = 0.056$ and 0.07 , respectively) (Figure 2b). Cortical thickness was significantly lower in both male and female NCX3^{-/-} mice, while the difference in bone volume fraction (BV/TV) was significant in females, but to a lesser extent in males ($p = 0.054$) (Figure 2b). Consistent with the μ CT results, femoral histomorphometry displayed significant decrease in trabecular bone volume and trabecular thickness while cortical bone appeared moderately thinner compared with sections from WT littermates (Figure 2c, Figure S3). Collectively, these findings demonstrated NCX3 contribution to mineral bone homeostasis in vivo.

3.2 | NCX3 deficiency impairs osteoblast mineralization in vitro

To better understand functional relevance of NCX3 gene in osteoblast mineralization in vitro, we employed CRISPR/Cas9 technology to inactivate SLC8A3 gene in MC3T3-E1 cells (Figure 3a). Compared to control cells, NCX3^{-/-} cells differentiated for 21 days in osteogenic conditions showed reduced Ca²⁺ deposition as assessed by Alizarin red staining (Figure 3b) and 50% reduction in quantitative Ca²⁺ deposition (Figure 3c). Interestingly, loss of NCX3 MC3T3-E1 cells also affected the expression of major markers of osteoblast differentiation such as *Runx2*, *Osx/Sp7*, *Alp (Alpl/Tnap)* and collagen *Colla1*, which suggested a broader role of this Na⁺/Ca²⁺ exchanger in transcriptional programming during osteoblast differentiation (Figure 3d). To further validate these observations and rule out any potential off-target effects of CRISPR/Cas9 targeting in MC3T3-E1 cells, we analyzed the

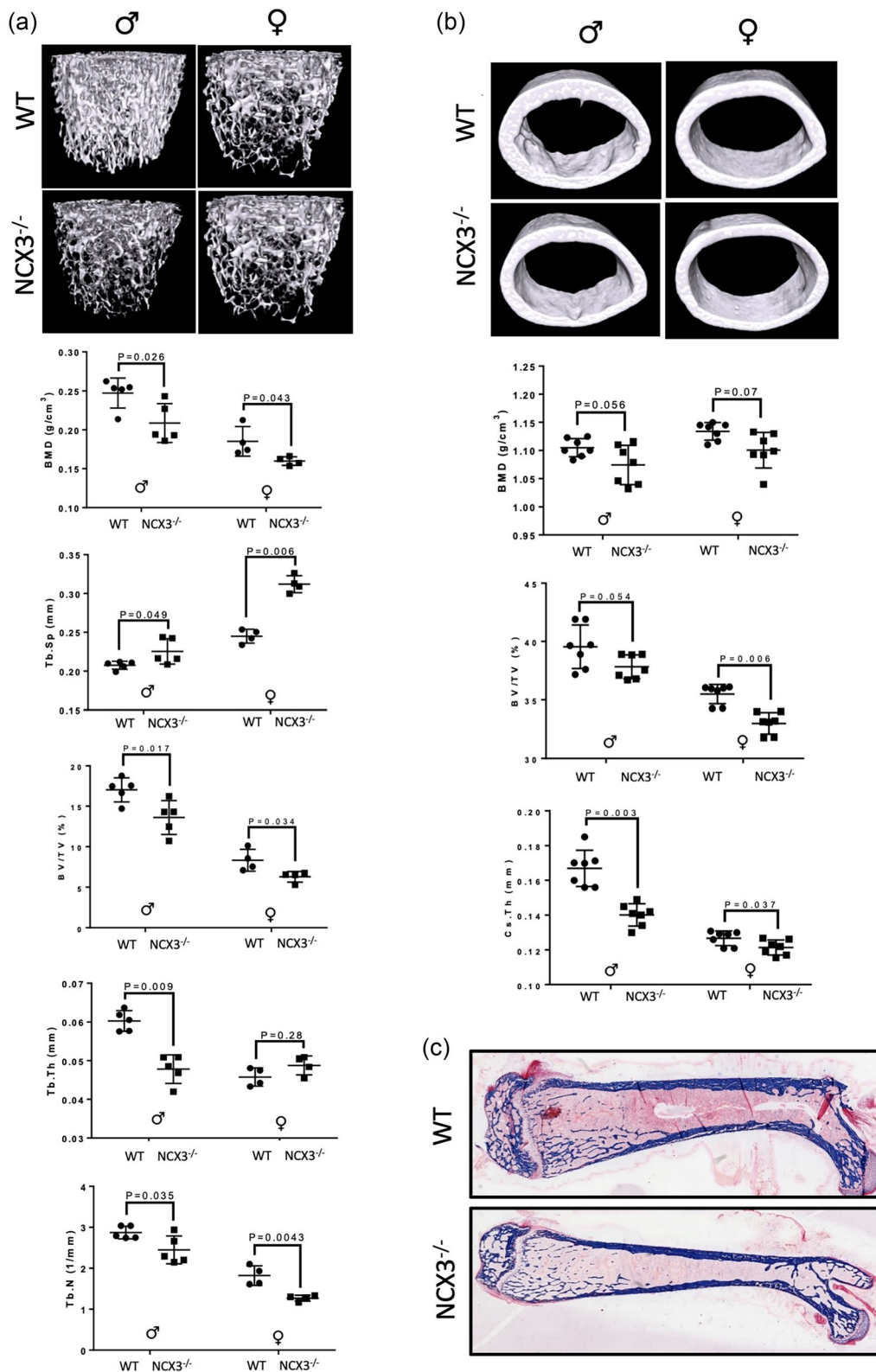


FIGURE 2 Decreased mineral bone density in NCX3^{-/-} mice. (a) Trabecular bone mineral density: representative μ CT images of femur, bone mineral density (BMD), trabecular space (Tb.Sp), bone volume per total volume (BV/TV), trabecular thickness (Tb.Th) and trabecular number (Tb.N) of 8-week-old male and female WT and NCX3^{-/-} mice. (b) Cortical bone density: representative μ CT images of femoral midshaft cortical bone of 8-week-old male and female WT and NCX3^{-/-} mice, cortical BMD, BV/TV, and cortical thickness (Cs/Th). (c) Representative Masson's trichrome-stained sections from femurs of 8 weeks old WT and NCX3^{-/-} mice. ($n = 4-5$ mice per genotype). Statistical significance was assessed using two-tailed Student's unpaired t -tests. Data are presented as the mean \pm SD (p -values indicated in graphs). NCX3, Na⁺/Ca²⁺ exchanger isoform-3; WT, wild type.

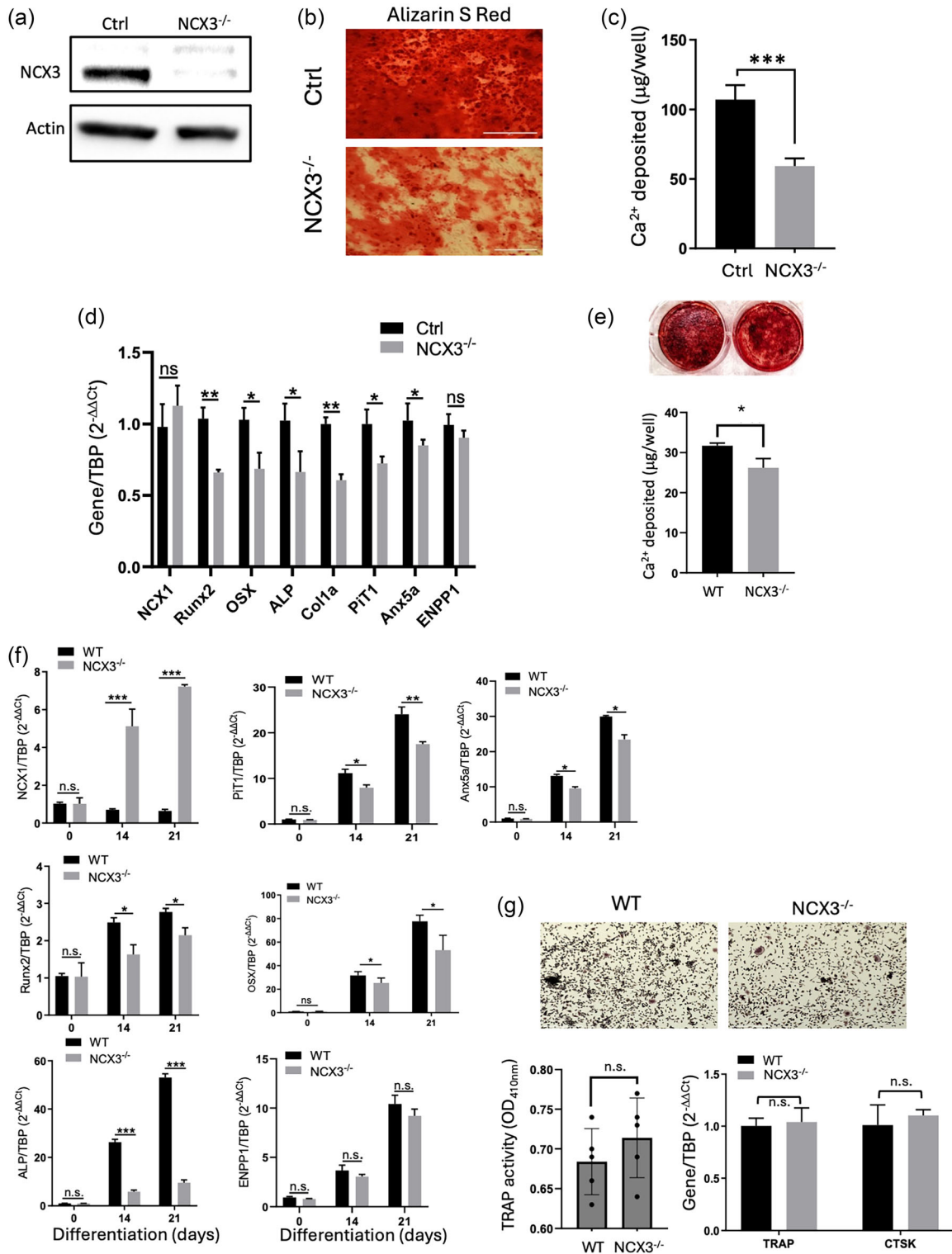


FIGURE 3 NCX3 is required for osteoblast mineralization in vitro. (a) Western blot verification of effective CRISPR-Cas9 knockout of *Slc8a3* gene in MC3T3-E1 osteoblasts. β -actin was used as a loading control. (b) Representative alizarin red staining and (c) quantification of Ca²⁺ deposition in control (Ctrl) and NCX3^{-/-} MC3T3-E1 osteoblasts grown for 21 days in osteogenic conditions ($n = 4$). (d) qRT-PCR analysis of PiT1, Anx5a, ENPP1 and selected osteogenic markers in control (Ctrl) and NCX3^{-/-} MC3T3-E1 osteoblasts grown for 21 days in osteogenic conditions. ($n = 3$). (e) Representative alizarin red staining and quantification of Ca²⁺ deposition in primary osteoblasts isolated from the calvarias of WT or NCX3^{-/-} mice. Cells were grown for 21 days in osteogenic conditions ($n = 3$). (f) qRT-PCR analysis of PiT1, ANXA5, ENPP1 and selected osteogenic markers in primary osteoblasts from WT or NCX3^{-/-} mice. (g) NCX3 deficiency does not affect osteoclast differentiation and function: representative images of TRAP staining, TRAP enzymatic activity, and qRT-PCR analysis of expression of osteoclast-associated genes (TRAP and CTSK) in primary osteoclasts derived from WT and NCX3^{-/-} mice. ($n = 3-5$). Statistical

(Continues)

FIGURE 3 (Continued)

significance was assessed using two-tailed Student's unpaired *t*-tests. Data are presented as the mean \pm SD ($*p < 0.05$, $**p < 0.01$, $***p < 0.001$, n.s.—not significant). Cas9, CRISPR-associated protein; CRISPR, Clustered Regularly Interspaced Short Palindromic Repeats; CTSK, cathepsin K; EPP1, ectonucleotide pyrophosphatase/phosphodiesterase 1; NCX3, Na⁺/Ca²⁺ exchanger isoform-3; qRT-PCR, quantitative real-time PCR; TRAP, tartrate-resistant acid phosphatase; SD, standard deviation; WT, wild type.

same parameters in primary osteoblasts isolated from calvaria of 3–5 days old WT and NCX3^{-/-} pups and cultured for 21 days under osteogenic conditions. Similarly, we observed reduced Alizarin red S staining intensity, reduced Ca²⁺ deposition, and a significant reduction in mRNA transcripts associated with osteoblastogenesis (*Runx2*, *Osx*, *Alp*) (Figure 3e,f). Interestingly, *Ncx1* mRNA expression was increased in NCX3-deficient primary osteoblasts (Figure 3f) and MC3T3-E1 cells (not shown), suggesting that NCX1 may play compensatory role in the absence of NCX3.

NCX1 and NCX3 are also expressed by osteoclasts (OC) and Li et al. (Li et al., 2007) showed they both contribute to osteoclastic pit formation. Limited growth of OCs in primary OB culture is to be expected, and required verification whether changes in OC activity could confound the in vivo results in NCX3^{-/-} mice. Therefore, we differentiated bone marrow-derived OCs from WT and NCX3^{-/-} mice using M-CSF followed by M-CSF+RANKL and measured tartrate-resistant acid phosphatase (TRAP) activity and assessed the expression of osteoclast marker genes cathepsin K (*Ctsk*) and *Trap* by real-time qRT-PCR. We observed no differences in OC differentiation or TRAP activity, thus indicating that NCX3 deficiency was unlikely to affect OC function (Figure 3g).

3.3 | NCX3 is present in osteoblast-derived matrix vesicles

A peptide signature consistent with NCX3 was identified by proteomic analysis with nanoflow reversed-phase liquid chromatography tandem mass spectrometry (nanoRPLC-MS/MS) of MVs derived from MC3T3-E1 pre-osteoblast (Xiao et al., 2007). Although the authors mistakenly described it as NCX2, the identified peptide KLTVEEEEAKRI has 100% coverage and identity with NCX3 of multiple species, mouse NCX3 isoform CRA_b and isoform 2 (GenBank: EDL02703.1 and NP_536688.2, respectively), and was assigned the correct Uniprot accession Q8VHJ8 (Xiao et al., 2007). Given the previously documented osteogenic functions of NCX3 and our own observations, we isolated MVs from the media of MC3T3-E1 cells grown under osteogenic conditions and characterized them by Nanosight Nanoparticle Tracking Analysis (NTA), immunogold labelling, and WB analysis. Compared to Day 0 (confluent cells prior to osteogenic differentiation), MV secretion significantly increased at Day 21 of osteogenic culture (Figure 4a). The size distribution of the isolated EVs was consistent with previously reported MV diameter range (Davies et al., 2019). Western blotting with MVs isolated from the media of differentiating MC3T3-E1 cells (Day 0, 14, and 21) also demonstrated NCX3 and PiT-1 protein expression, increasing with osteogenic differentiation. Since there is no accepted MV marker protein capable of serving as a loading control, we used membrane staining by Ponceau S as evidence of even loading (Figure 4b). We next performed immunogold labelling of NCX3 in mineralizing osteoblasts, with TEM focused on the area of MV budding off the plasma membrane (Figure 4c) and observed a clear NCX3 signal indicated by red arrows (Figure 4c, right panel). Control immunogold staining without the primary antibody did not demonstrate any signal (not shown). Furthermore, IF images of differentiated primary human osteoblasts showed abundant expression of NCX3 protein in vesicular compartments and in extracellular structures of similar diameter as the MVs (Figure 4d, left and centre panels). We also observed a similar pattern of NCX3 expression in decalcified mouse femurs (Figure 4d, right panel). These redundant observations confirm NCX3 expression in mineralizing MVs.

3.4 | Loss of NCX3 impairs MV Ca²⁺ entry and MV-mediated mineralization in vitro

We employed scanning electron microscopy coupled with Energy Dispersive Spectroscopy (SEM-EDS) to examine the impact of NCX3 loss on the calcium-to-phosphate (Ca/P) ratio within the MVs isolated from mineralizing control or NCX3^{-/-} MC3T3-E1 osteoblasts (Figure 5a–c). In mature hydroxyapatite (HA), the approximate Ca/P ratio is 1.6, though the composition of amorphous calcium phosphate in MVs can vary, leading to the observed range of 1.43 ± 0.09 . The absence of NCX3 was associated with a reduction in the relative abundance of Ca²⁺ within the isolated MVs ($p = 0.0049$; see Figure 5d). To further assess the intrinsic mineralization efficacy of isolated MVs, we conducted a cell-free in vitro MV-collagen calcification assay under osteogenic conditions utilizing MVs harvested from control and NCX3^{-/-} MC3T3-E1 cells cultured in osteogenic conditions for 21 days. These MVs were then seeded on type I collagen-coated glass coverslips and exposed to osteogenic media for 72 h. Quantitative analysis using a colorimetric Ca²⁺ assay revealed a significantly diminished ability of MVs from NCX3^{-/-} MC3T3-E1 cells to promote calcification (Figure 5e). These observations suggest that NCX3 is necessary for the optimal Ca²⁺ transport and the initial content of amorphous hydroxyapatite in MVs, and that NCX3 significantly contributes to establishing the critical mass of hydroxyapatite within the MV lumen and to MV-mediated collagen mineralization.

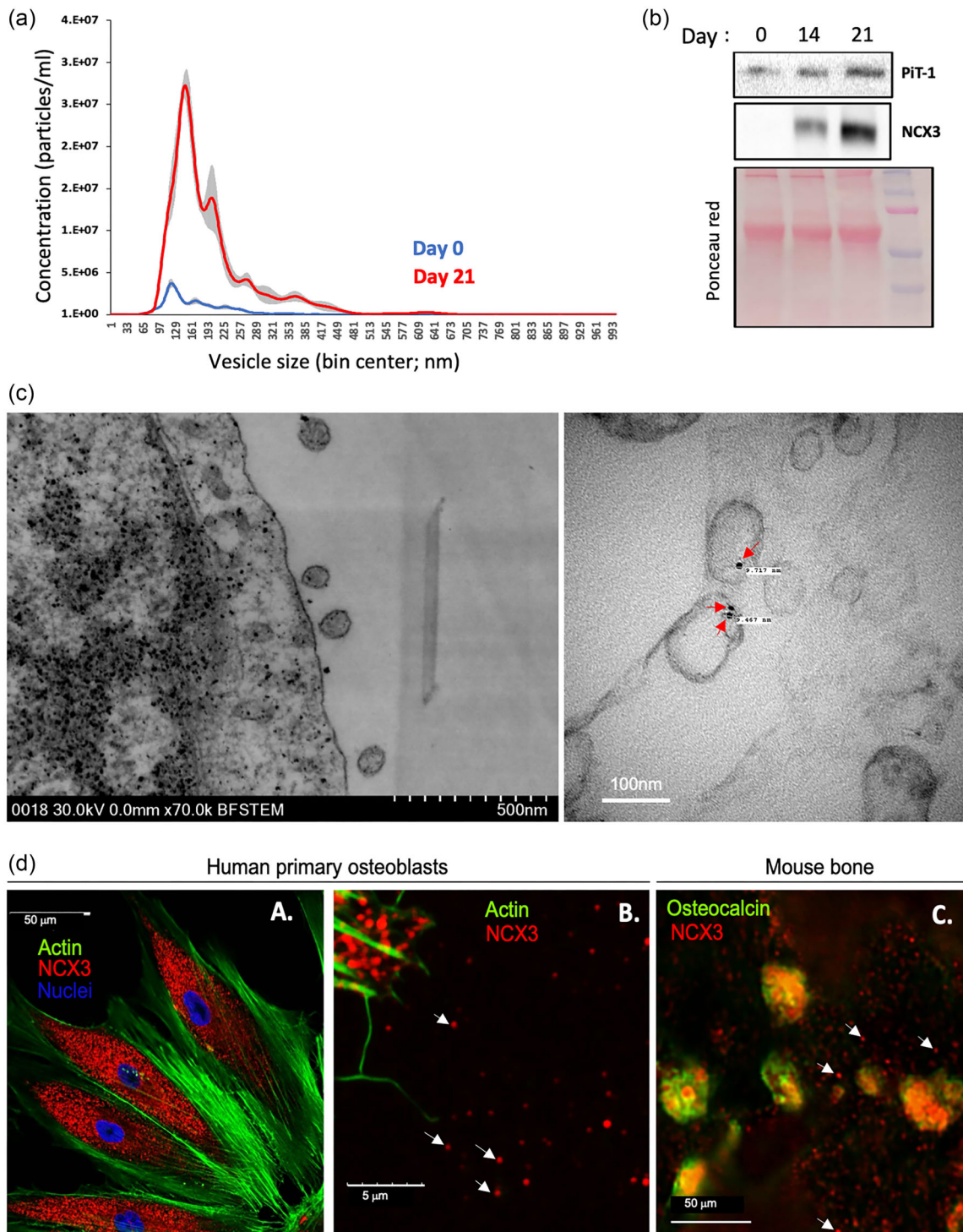


FIGURE 4 NCX3 is expressed in osteoblast-derived matrix vesicles (MV). (a) NTA histogram depicting the size distribution of microvesicles purified from the media of MC3T3-E1 cell culture on Day 0 (confluence; blue tracing) and Day 21 of post-confluent osteogenic culture (red tracing). Grey areas indicate SEM ($n = 5-8$). (b) TEM immunogold labelling of NCX3 (black 10 nm dots) in the intracellular compartment (lower magnification in the left panel) and in budding MVs of mineralizing MC3T3-E1 cells (higher magnification in the right panel; red arrows indicate NCX3 immunogold labelling). (c) Western blot analysis of the expression of PiT1 and NCX3 proteins in the MVs isolated from MC3T3-E1 cell culture supernatants on Day 0, Day 14 and Day 21 of osteogenic culture. Ponceau S staining was used to demonstrate even protein loading ($n = 3$). (d) Confocal imaging of NCX3 expression in human primary osteoblasts (NCX3 in red, actin in green, nuclei in blue) and in the mouse bone (NCX3 in red, osteocalcin in green). White arrowheads indicate selected extracellular punctate staining within extracellular vesicular compartment. ($n = 3$). NCX3, Na⁺/Ca²⁺ exchanger isoform-3; NTA, nanoparticle tracking analysis; SEM, scanning electron microscopy.

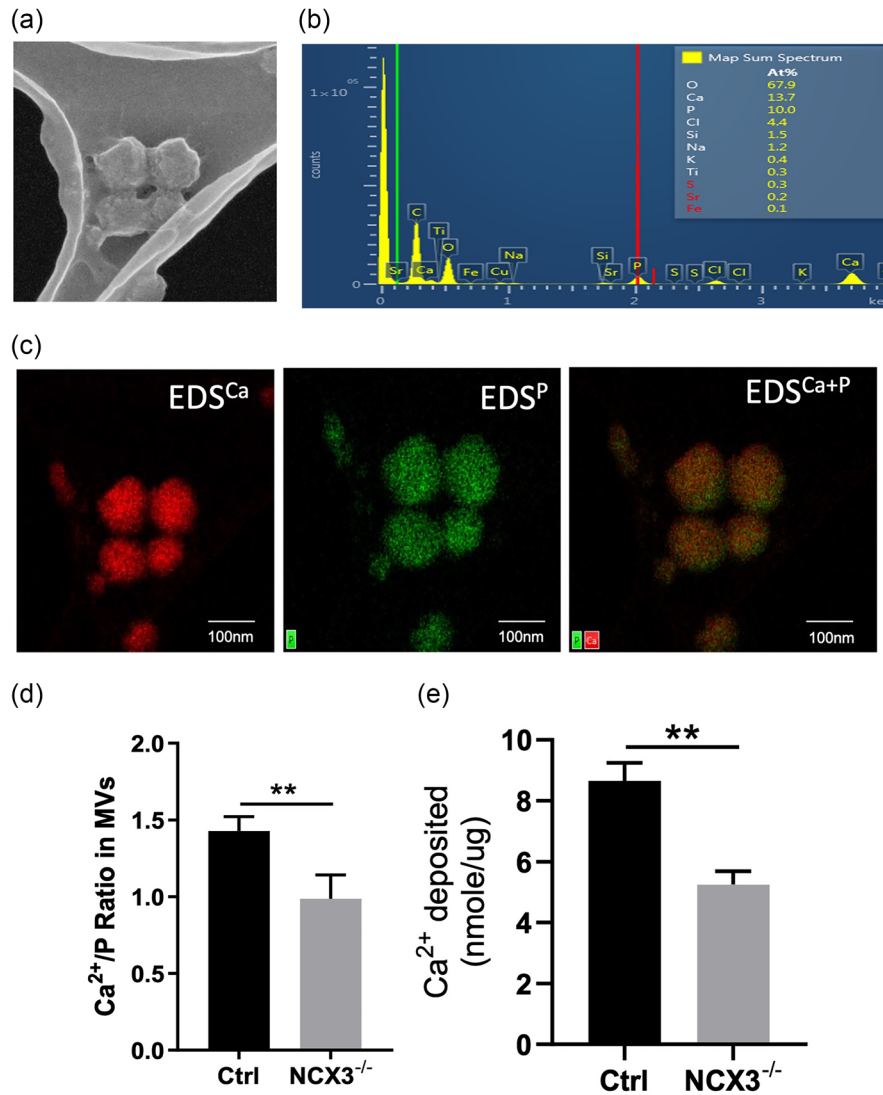


FIGURE 5 NCX3 determines Ca²⁺ content in MVs and their ability to direct mineralization in vitro. (a) Representative SEM image of MVs deposited on the copper grid. (b) Representative elemental composition of the MV content from SEM-EDS analysis. (c) Representative imaging of calcium (red) and phosphorus (green) and their overlay using SEM-EDS. (d) Ca/P ratio analyzed by SEM-EDS in MVs isolated from the media of Ctrl and NCX3^{-/-} MC3T3-E1 cells harvested on Day 21 of osteogenic growth. ($n = 3-4$). (e) Cell-free in vitro MV-collagen calcification assay with MVs isolated from Ctrl and NCX3^{-/-} MC3T3-E1 osteoblasts. ($n = 3$). Statistical significance was assessed using two-tailed Student's unpaired *t*-tests. Data are presented as the mean \pm SD (** $p < 0.01$). MV, matrix vesicles; NCX3, Na⁺/Ca²⁺ exchanger isoform-3; SD, standard deviation; SEM-EDS, scanning electron microscopy coupled with Energy Dispersive Spectroscopy.

3.5 | NCX3 is a target of mediators associated with chronic inflammation

During conditions of persistent inflammation such as rheumatoid arthritis, inflammatory bowel diseases, chronic liver diseases and other chronic inflammatory disorders, decoupling of osteoblast and osteoclast activities contributes to a defect in bone remodelling leading to osteopenia and osteoporosis (Epsley et al., 2020; Ghishan & Kiela, 2011; Tilg et al., 2008). We investigated the effects of inflammatory cytokines on the expression of NCX3 in osteoblasts. Compared to a later timepoints, early exposure to TNF in osteoblast culture leads to a more profound inhibition of mineralization (Gilbert et al., 2000), which would dramatically affect the yields of MVs and make the results difficult to interpret. The 72 h exposure time was chosen for two reasons: to be more representative of chronic inflammation, and to allow for adequate accumulation of MVs in the media which would permit their isolation and downstream assays (24 h period was not sufficient). Under these conditions, TNF α , IL1 β , or IFN γ treatment of differentiated MC3T3-E1 cells significantly decreased NCX3 protein expression (Figure 6a). TNF α also reduced NCX3 mRNA expression in differentiated primary human osteoblasts (Figure 6b). TNF α also suppressed NCX3 expression in MVs, as demonstrated by western blot analysis of MVs isolated from the osteogenic culture media of MC3T3-E1 cells treated with or without the cytokine (Figure 6c). To test the effects of chronic inflammation on bone NCX3 expression in vivo, we used the model of chronic dextran sulphate sodium (DSS)-induced colitis in mice by administering 2.5% DSS in three cycles (7 days on, 14 days off).

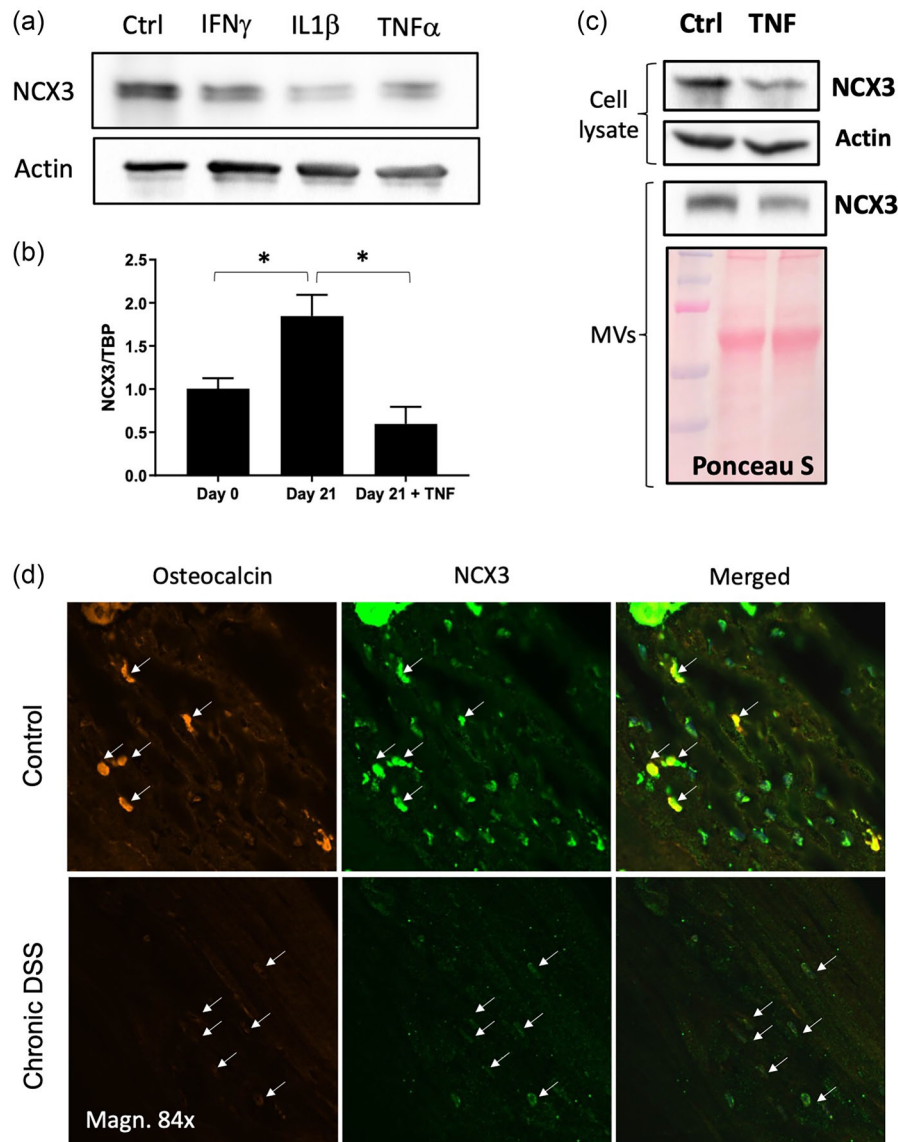


FIGURE 6 Total and MV-associated NCX3 is a target of inhibition by inflammatory mediators in vitro and in vivo. (a) Western blotting analysis of NCX3 protein expression in the cell lysate of primary mouse osteoblasts after treatment with various proinflammatory cytokines (IFN γ (100U/mL), IL1 β (10 ng/mL) and TNF α (10 ng/mL) in the last 72 h of 21-day osteogenic differentiation. β -actin was used as a loading control. (representative of $n = 3$). (b) qRT-PCR analysis of NCX3 mRNA expression in primary human osteoblasts on Day 0 (confluence, Day 21 of osteogenic culture, and after treatment with 10 ng/mL TNF α in the last 72 hours of osteogenic differentiation. ($n = 3$). Statistical significance was assessed using two-tailed Student's unpaired t tests. Data are presented as the mean \pm SD ($*p < 0.05$). (c) Western blot analysis of NCX3 protein expression in the total cell lysate and MVs derived from MC3T3-E1 cells after treatment with TNF α (10 ng/mL) in the last 72 h of 21-day osteogenic culture. β -actin and Ponceau S staining were used as loading controls for the cell lysates and MVs, respectively ($n = 3$). (d) IF images of NCX3 expression in decalcified femurs isolated from healthy mice and mice with chronic colitis. Arrows indicate osteocalcin-positive osteoblasts (representative of $n = 4$). MV, matrix vesicle; NCX3, Na $^{+}$ /Ca $^{2+}$ exchanger isoform-3; qRT-PCR, quantitative real-time PCR.

Immunofluorescence analysis of NCX3 and osteocalcin (as an OB marker) protein expression in demineralized femurs displayed diminished expression of NCX3 colocalized with osteocalcin in colitic mice (Figure 6d). Consistent with human and mouse data (Abitbol et al., 1995; Bischoff et al., 1997; Dresner-Pollak et al., 2004; Larmonier et al., 2013), osteocalcin expression was also decreased. Therefore, images acquired with higher exposure/gain had to be used to mark localization of osteocalcin-positive OBs (arrows). However, representative images presented in Figure 6d use identical image acquisition settings in both control and DSS-treated mice, thus osteocalcin signal is very weak in the latter group.

4 | DISCUSSION

During the process of bone formation, osteoblasts promote mineralization by releasing membrane enclosed submicroscopic MVs which provide initial seeding site for nucleation and formation of HA (Bommanavar et al., 2020). MV membrane is equipped

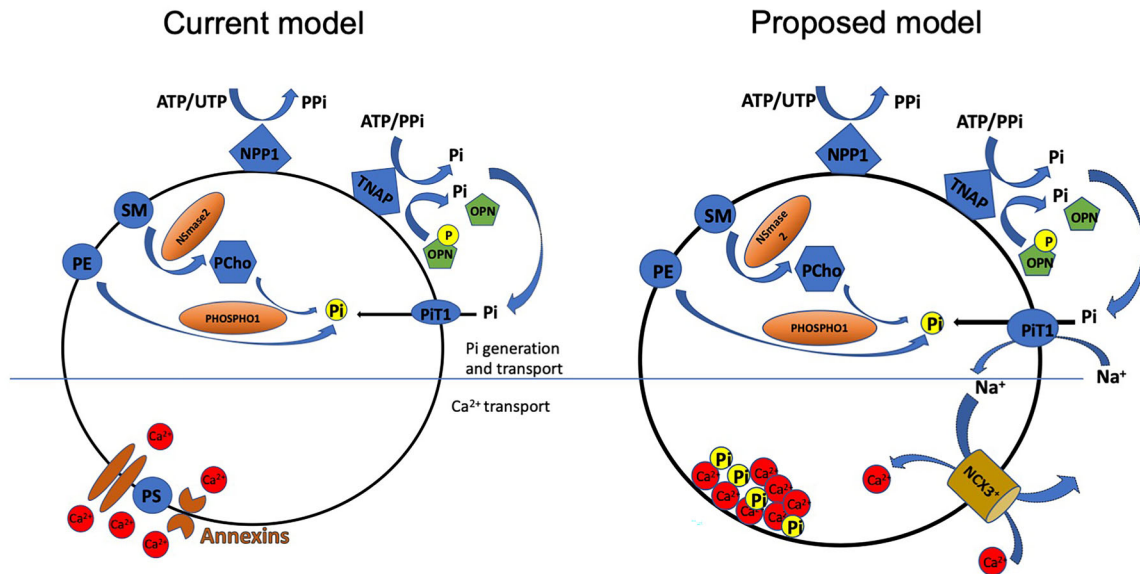


FIGURE 7 Current and proposed model of Pi and Ca^{2+} transport in matrix vesicles. PS – phosphatidylserine; PE – phosphoethanolamine, PCho – phosphocholine; SM – sphingomyelin; PPI – inorganic pyrophosphate; Pi – inorganic phosphate; ATP – adenosine triphosphate; UTP – uridine triphosphate; PHOSPHO1 – phosphoethanolamine/phosphocholine phosphatase 1; NSmase2 – SMPD3; sphingomyelin phosphodiesterase 3; NPP1 – ENPP1, ectonucleotide pyrophosphatase/phosphodiesterase 1; TNAP – ALPL, biominerization associated alkaline phosphatase; OPN – SPPI, osteopontin, secreted phosphoprotein 1; Pit1 – GLVRI, SLC20A1, solute carrier family 20 member 1; NCX3 – solute carrier family 8 (sodium/calcium exchanger), member 3, SLC8A3.

with enzymes, ion channels and transporters that function synchronously to facilitate accumulation of Ca^{2+} and Pi within MV lumen (Boyan et al., 2022; Davies, 2023; Hasegawa et al., 2022). Although the mechanism and proteins involved in intravesicular supply of Pi is relatively well known, the source and transport mechanism of Ca^{2+} across the MVs membrane remains poorly characterized and controversial. Previous studies identified NCX3 as the major Ca^{2+} efflux mediator that supplies Ca^{2+} out of osteoblasts into mineralizing bone matrix and $\text{Na}^+/\text{Ca}^{2+}$ exchanger inhibitor resulted in impaired Ca^{2+} deposition at mineralization sites (Sosnoski & Gay, 2008; Stains & Gay, 1998; Stains et al., 2002). However, its presence or functional role in MVs was not previously studied, even after the role of annexins in mediating Ca^{2+} transport in MVs was brought into question (Belluoccio et al., 2010; Blandford et al., 2003). Our study implicates a direct role of NCX3 in MVs required for normal bone homeostasis. This conclusion is based on the following observations: (a) NCX3 expression increases with osteogenic differentiation in mouse pre-osteoblasts, (b) loss of NCX3 in vivo and in vitro impairs osteoblast mineralization, (c) NCX3 protein is present in the MV membrane, and within MVs, (d) NCX3 significantly contributes to Ca^{2+} accumulation and MV-directed Ca^{2+} deposition within the collagen matrix. We also describe that NCX3 is a target of negative regulation by inflammatory cytokines associated with chronic inflammation, suggesting that its suppressed expression and/or activity may contribute to inflammation-associated osteopenia and osteoporosis.

Considering the ability of NCX3 to function as a bi-directional exchanger, depending on the established Na^+ gradient, Sosnoski and Gay (Sosnoski & Gay, 2008) showed that NCX3 contributed to the Ca^{2+} uptake and efflux in MC3T3-E1 osteoblasts and concluded that NCX3 “functions as the major portal for translocation of calcium ions into sites of mineralization”. Using multiple approaches, our work confirms and extends our understanding of the roles NCX3 plays in bone mineralization. Although NCX3^{-/-} mice were anatomically indistinguishable from wild type mice, with no overt skeletal abnormalities, femoral μCT analysis and bone histomorphometry revealed measurable deficiencies in NCX3^{-/-} mice. Except for trabecular thickness, which was not affected in NCX3^{-/-} females, all other parameters of trabecular bone were reduced in both sexes at 8 weeks of age. Cortical bone was also negatively affected by NCX3 deficiency, though not to the same extent as trabecular bone. The less pronounced effect of NCX3 knockout on cortical BMD may reflect the unique structural and metabolic properties of cortical versus trabecular bone. While the trabecular bone is characterized by its high surface to volume ratio, is more metabolically active and displays heightened sensitivity to impaired Ca^{2+} metabolism, cortical bone has dense and compact structure and is less metabolically active (Clarke, 2008). Interestingly, differences in bone parameters became less pronounced with age (24 weeks), suggesting that compensatory mechanisms may be activated over time. It is plausible that NCX1 isoform could provide such compensation since we observed a gradual increase in its expression in differentiating NCX3-deficient primary mouse osteoblasts (Figure 3f).

NCX3 is also expressed in osteoclasts (Albano et al., 2017; Li et al., 2007) and its knockdown or pharmacological inhibition of $\text{Na}^+/\text{Ca}^{2+}$ exchange in primary mouse osteoclasts suppressed osteoclastic pit formation (Li et al., 2007). Therefore, we considered whether the observed bone phenotype in NCX3^{-/-} mice could be confounded by changes in osteoclast function. However, osteoclasts isolated from NCX3^{-/-} mice displayed no difference in their TRAP activity and osteoclast marker genes such as

TRAP and Cathepsin K when compared with WT mice. Although this data does not support the role of NCX3 in osteoclast differentiation and function, if NCX3 deficiency in osteoclast could indeed negatively affect bone resorption, the observed net effects on bone parameters in our μ CT and histomorphometric analyses would suggest an underestimated importance of NCX3 in osteoblast-driven mineralization. This could be addressed in the future through the targeted deletion of NCX3 specifically in osteoblasts and/or osteoclasts.

Chronic intestinal inflammation is associated with impaired Ca^{2+} homeostasis at multiple levels, from vitamin D metabolism (Ghishan & Kiela, 2011; Ghishan & Kiela, 2017), reduced dietary Ca^{2+} intake (Silvennoinen et al., 1996), impaired intestinal absorption (Huybers et al., 2008), to urinary Ca^{2+} wasting (Breuer et al., 1970; Radhakrishnan et al., 2013). Similar to our previous observations that renal NCX1 is downregulated by $\text{IFN}\gamma$ during experimental colitis, leading to reduced Ca^{2+} reabsorption and a negative systemic Ca^{2+} balance (Radhakrishnan et al., 2015), NCX3 also appears to be a target of inhibition by inflammatory mediators associated with Inflammatory Bowel Disease (IBD) in osteoblasts, including NCX3 expression in MVs. This implies that the NCX3-dependent component of Ca^{2+} utilization by osteoblasts during early steps of mineralization is also affected by chronic inflammatory disorders and that this mechanism likely contributes to the complex mechanisms underlying bone loss in chronic inflammation. Interestingly, the role of NCX3 may go beyond its direct involvement in Ca^{2+} flux, since its loss in MC3T3-E1 cells or primary murine osteoblasts also resulted in a significant reduction in major mineralization markers such as Runx2, alkaline phosphatase (ALP), osterix (OSX), and even collagen 1a. This may further impact osteoblast differentiation and function, although the precise mechanism(s) involved remain to be elucidated.

In summary, our findings confirm the evidence of NCX3 expression in osteoblast-derived MVs and its contribution to MV-mediated mineralization. The functional importance of NCX3 and its co-expression with PiT-1 in differentiating osteoblasts and MVs have led us to propose a novel model of Ca^{2+} and Pi transport in MVs (Figure 7), whereby coupled activities of Na^+ /Pi co-transport and Na^+ / Ca^{2+} exchange may provide the major route for the transport of Pi and Ca^{2+} into MV lumen to promote HA synthesis during primary mineralization.

AUTHOR CONTRIBUTIONS

Irshad A. Sheikh: Data curation; formal analysis; investigation; methodology; writing—original draft. **Monica T. Midura-Kiela:** Investigation; resources; writing—review and editing. **André Herchuelz:** Resources; writing—review and editing. **Sophie Sokolow:** Resources; writing—review and editing. **Pawel R. Kiela:** Conceptualization; investigation; project administration; resources; supervision; validation; visualization; writing—review and editing. **Fayez K. Ghishan:** Conceptualization; funding acquisition; project administration; resources; writing—review and editing.

ACKNOWLEDGEMENTS

We thank Yao-Jen Chang at Kuiper Imaging Facility of University of Arizona for providing technical support with EDS imaging and analysis. William A. Day at the AHSC Electron Microscope Core Facility of University of Arizona for his help with immunogold labelling and EM imaging. Shoshana Yakar from Department of Molecular Pathobiology, New York University College of Dentistry and Johanna Warshaw from Department of Basic Science & Craniofacial Biology, NYU College of Dentistry for assistance in μ CT analysis and static histomorphometry.

CONFLICT OF INTEREST STATEMENT

The authors declare no conflicts of interest.

ORCID

Pawel R. Kiela  <https://orcid.org/0000-0002-0014-3517>

REFERENCES

- Abitbol, V., Roux, C., Chaussade, S., Guillemant, S., Kolta, S., Dougados, M., Couturier, D., & Amor, B. (1995). Metabolic bone assessment in patients with inflammatory bowel disease. *Gastroenterology*, 108, 417–422. [https://doi.org/10.1016/0016-5085\(95\)90068-3](https://doi.org/10.1016/0016-5085(95)90068-3)
- Albano, G., Dolder, S., Siegrist, M., Mercier-Zuber, A., Auberson, M., Stoudmann, C., Hofstetter, W., Bonny, O., & Fuster, D. G. (2017). Increased bone resorption by osteoclast-specific deletion of the sodium/calcium exchanger isoform 1 (NCX1). *Pflugers Archive: European Journal of Physiology*, 469, 225–233. <https://doi.org/10.1007/s00424-016-1923-5>
- Anderson, H. C., Garimella, R., & Tague, S. E. (2005). The role of matrix vesicles in growth plate development and biomineralization. *Frontiers in Bioscience: A Journal and Virtual Library*, 10, 822–837. <https://doi.org/10.2741/1576>
- Ansari, S., de Wildt, B. W. M., Vis, M. A. M., de Korte, C. E., Ito, K., Hofmann, S., & Yuana, Y. (2021). Matrix vesicles: Role in bone mineralization and potential use as therapeutics. *Pharmaceuticals*, 14, 289. <https://doi.org/10.3390/ph14040289>
- Belluoccio, D., Grskovic, I., Niehoff, A., Schlötzer-Schrehardt, U., Rosenbaum, S., Etich, J., Frie, C., Pausch, F., Moss, S. E., Pöschl, E., Bateman, J. F., & Brachvogel, B. (2010). Deficiency of annexins A5 and A6 induces complex changes in the transcriptome of growth plate cartilage but does not inhibit the induction of mineralization. *Journal of Bone and Mineral Research: The Official Journal of the American Society for Bone and Mineral Research*, 25, 141–153. <https://doi.org/10.1359/jbmr.090710>
- Bischoff, S. C., Herrmann, A., Göke, M., Manns, M. P., Von zur Mühlen, A., & Brabant, G. (1997). Altered bone metabolism in inflammatory bowel disease. *American Journal of Gastroenterology*, 92, 1157–1163.

- Blandford, N. R., Sauer, G. R., Genge, B. R., Wu, L. N., & Wuthier, R. E. (2003). Modeling of matrix vesicle biomineralization using large unilamellar vesicles. *Journal of Inorganic Biochemistry*, 94, 14–27. [https://doi.org/10.1016/s0162-0134\(02\)00629-3](https://doi.org/10.1016/s0162-0134(02)00629-3)
- Bommanavar, S., Hosmani, J., Togoo, R. A., Baeshen, H. A., Raj, A. T., Patil, S., Bhandi, S., & Birkhed, D. (2020). Role of matrix vesicles and crystal ghosts in bio-mineralization. *Journal of Bone and Mineral Metabolism*, 38(6), 759–764. <https://doi.org/10.1007/s00774-020-01125-x>
- Bottini, M., Mebarek, S., Anderson, K. L., Strzelecka-Kiliszek, A., Bozycki, L., Simão, A. M. S., Bolean, M., Ciancaglini, P., Pikula, J. B., Pikula, S., Magne, D., Volkman, N., Hanein, D., Millán, J. L., & Buchet, R. (2018). Matrix vesicles from chondrocytes and osteoblasts: Their biogenesis, properties, functions and biomimetic models. *Biochimica et Biophysica Acta. General subjects*, 1862, 532–546. <https://doi.org/10.1016/j.bbagen.2017.11.005>
- Boyan, B. D., Asmussen, N. C., Lin, Z., & Schwartz, Z. (2022). The role of matrix-bound extracellular vesicles in the regulation of endochondral bone formation. *Cells*, 11, 1619. <https://doi.org/10.3390/cells11101619>
- Breuer, R. I., Gelzayd, E. A., & Kirsner, J. K. (1970). Urinary crystalloid excretion in patients with inflammatory bowel disease. *Gut*, 11, 314–318. <https://doi.org/10.1136/gut.11.4.314>
- Chen, N. X., Kircelli, F., O'Neill, K. D., Chen, X., & Moe, S. M. (2010). Verapamil inhibits calcification and matrix vesicle activity of bovine vascular smooth muscle cells. *Kidney International*, 77, 436–442. <https://doi.org/10.1038/ki.2009.481>
- Chen, N. X., O'Neill, K. D., Chen, X., & Moe, S. M. (2008). Annexin-mediated matrix vesicle calcification in vascular smooth muscle cells. *Journal of Bone and Mineral Research: The Official Journal of the American Society for Bone and Mineral Research*, 23, 1798–1805. <https://doi.org/10.1359/jbmr.080604>
- Clarke, B. (2008). Normal bone anatomy and physiology. *Clinical journal of the American Society of Nephrology: CJASN*, 3(Suppl 3), S131–S139. <https://doi.org/10.2215/CJN.04151206>
- Connerty, H. V., & Briggs, A. R. (1966). Determination of serum calcium by means of orthocresolphthalein complexone. *American Journal of Clinical Pathology*, 45, 290–296. <https://doi.org/10.1093/ajcp/45.3.290>
- Dai, Q., Han, Y., Xie, F., Ma, X., Xu, Z., Liu, X., Zou, W., & Wang, J. (2018). A RANKL-based osteoclast culture assay of mouse bone marrow to investigate the role of mTORC1 in osteoclast formation. *Journal of Visualized Experiments: JoVE*, 56468(133), 56486. <https://doi.org/10.3791/56468>
- D'Angelo, M., Billings, P. C., Pacifici, M., Leboy, P. S., & Kirsch, T. (2001). Authentic matrix vesicles contain active metalloproteases (MMP). A role for matrix vesicle-associated MMP-13 in activation of transforming growth factor-beta. *The Journal of Biological Chemistry*, 276, 11347–11353. <https://doi.org/10.1074/jbc.M009725200>
- Davies, O. G. (2023). Extracellular vesicles: From bone development to regenerative orthopedics. *Molecular Therapy: The Journal of the American Society of Gene Therapy*, 31, 1251–1274. <https://doi.org/10.1016/j.ymthe.2023.02.021>
- Davies, O. G., Cox, S. C., Azoidis, I., McGuinness, A. J. A., Cooke, M., Heaney, L. M., Davis, E. T., Jones, S. W., & Grover, L. M. (2019). Osteoblast-derived vesicle protein content is temporally regulated during osteogenesis: implications for regenerative therapies. *Frontiers in Bioengineering and Biotechnology*, 7, 92. <https://doi.org/10.3389/fbioe.2019.00092>
- Dresner-Pollak, R., Gelb, N., Rachmilewitz, D., Karmeli, F., & Weinreb, M. (2004). Interleukin 10-deficient mice develop osteopenia, decreased bone formation, and mechanical fragility of long bones. *Gastroenterology*, 127, 792–801. <https://doi.org/10.1053/j.gastro.2004.06.013>
- Epsley, S., Tadros, S., Farid, A., Kargilis, D., Mehta, S., & Rajapakse, C. S. (2020). The effect of inflammation on bone. *Frontiers in Physiology*, 11, 511799. <https://doi.org/10.3389/fphys.2020.511799>
- Ghishan, F. K., & Kiela, P. R. (2011). Advances in the understanding of mineral and bone metabolism in inflammatory bowel diseases. *American Journal of Physiology: Gastrointestinal and Liver Physiology*, 300, G191–G201. <https://doi.org/10.1152/ajpgi.00496.2010>
- Ghishan, F. K., & Kiela, P. R. (2017). Vitamins and minerals in inflammatory bowel disease. *Gastroenterology Clinics of North America*, 46, 797–808. <https://doi.org/10.1016/j.gtc.2017.08.011>
- Gilbert, L., He, X., Farmer, P., Boden, S., Kozlowski, M., Rubin, J., & Nanes, M. S. (2000). Inhibition of osteoblast differentiation by tumor necrosis factor-alpha. *Endocrinology*, 141, 3956–3964. <https://doi.org/10.1210/endo.141.11.7739>
- Golub, E. E. (2009). Role of matrix vesicles in biomineralization. *Biochimica et Biophysica Acta*, 1790, 1592–1598. <https://doi.org/10.1016/j.bbagen.2009.09.006>
- Hasegawa, T. (2018). Ultrastructure and biological function of matrix vesicles in bone mineralization. *Histochemistry and Cell Biology*, 149, 289–304. <https://doi.org/10.1007/s00418-018-1646-0>
- Hasegawa, T., Hongo, H., Yamamoto, T., Abe, M., Yoshino, H., Haraguchi-Kitakamae, M., Ishizu, H., Shimizu, T., Iwasaki, N., & Amizuka, N. (2022). Matrix vesicle-mediated mineralization and osteocytic regulation of bone mineralization. *International Journal of Molecular Sciences*, 23, 9941. <https://doi.org/10.3390/ijms23179941>
- Huybers, S., Apostolaki, M., van der Eerden, B. C., Kollias, G., Naber, T. H., Bindels, R. J., & Hoenderop, J. G. (2008). Murine TNF(DeltaARE) Crohn's disease model displays diminished expression of intestinal Ca²⁺ transporters. *Inflammatory Bowel Diseases*, 14, 803–811. <https://doi.org/10.1002/ibd.20385>
- Johnson, K., Moffa, A., Chen, Y., Pritzker, K., Goding, J., & Terkeltaub, R. (1999). Matrix vesicle plasma cell membrane glycoprotein-1 regulates mineralization by murine osteoblastic MC3T3 cells. *Journal of Bone and Mineral Research: The Official Journal of the American Society for Bone and Mineral Research*, 14, 883–892. <https://doi.org/10.1359/jbmr.1999.14.6.883>
- Kirsch, T. (2005). Annexins—Their role in cartilage mineralization. *Frontiers in Bioscience: A Journal and Virtual Library*, 10, 576–581. <https://doi.org/10.2741/1553>
- Kirsch, T., Ishikawa, Y., Mwale, F., & Wuthier, R. E. (1994). Roles of the nucleational core complex and collagens (types II and X) in calcification of growth plate cartilage matrix vesicles. *The Journal of Biological Chemistry*, 269, 20103–20109.
- Kirsch, T., Nah, H. D., Shapiro, I. M., & Pacifici, M. (1997). Regulated production of mineralization-competent matrix vesicles in hypertrophic chondrocytes. *The Journal of Cell Biology*, 137, 1149–1160. <https://doi.org/10.1083/jcb.137.5.1149>
- Larmonier, C. B., McFadden, R. M., Hill, F. M., Schreiner, R., Ramalingam, R., Besselsen, D. G., Ghishan, F. K., & Kiela, P. R. (2013). High vitamin D3 diet administered during active colitis negatively affects bone metabolism in an adoptive T cell transfer model. *American Journal of Physiology: Gastrointestinal and Liver Physiology*, 305, G35–G46. <https://doi.org/10.1152/ajpgi.00065.2013>
- Leach, R. J., Schwartz, Z., Johnson-Pais, T. L., Dean, D. D., Luna, M., & Boyan, B. D. (1995). Osteosarcoma hybrids can preferentially target alkaline phosphatase activity to matrix vesicles: evidence for independent membrane biogenesis. *Journal of Bone and Mineral Research: The Official Journal of the American Society for Bone and Mineral Research*, 10, 1614–1624. <https://doi.org/10.1002/jbmr.5650101103>
- Li, J. P., Kajiyama, H., Okamoto, F., Nakao, A., Iwamoto, T., & Okabe, K. (2007). Three Na⁺/Ca²⁺ exchanger (NCX) variants are expressed in mouse osteoclasts and mediate calcium transport during bone resorption. *Endocrinology*, 148, 2116–2125. <https://doi.org/10.1210/en.2006-1321>
- McLeod, M. J. (1980). Differential staining of cartilage and bone in whole mouse fetuses by alcian blue and alizarin red S. *Teratology*, 22, 299–301. <https://doi.org/10.1002/tera.1420220306>
- Minamizaki, T., Nakao, Y., Irie, Y., Ahmed, F., Itoh, S., Sarmin, N., Yoshioka, H., Nobukiyo, A., Fujimoto, C., Niida, S., Sotomaru, Y., Tanimoto, K., Kozai, K., Sugiyama, T., Bonnelye, E., Takei, Y., & Yoshiko, Y. (2020). The matrix vesicle cargo miR-125b accumulates in the bone matrix, inhibiting bone resorption in mice. *Communications Biology*, 3, 30. <https://doi.org/10.1038/s42003-020-0754-2>

- Nahar, N. N., Missana, L. R., Garimella, R., Tague, S. E., & Anderson, H. C. (2008). Matrix vesicles are carriers of bone morphogenetic proteins (BMPs), vascular endothelial growth factor (VEGF), and noncollagenous matrix proteins. *Journal of Bone and Mineral Metabolism*, 26, 514–519. <https://doi.org/10.1007/s00774-008-0859-z>
- Radhakrishnan, V. M., Kojs, P., Ramalingam, R., Midura-Kiela, M. T., Angeli, P., Kiela, P. R., & Ghishan, F. K. (2015). Experimental colitis is associated with transcriptional inhibition of Na⁺/Ca²⁺ exchanger isoform 1 (NCX1) expression by interferon γ in the renal distal convoluted tubules. *The Journal of Biological Chemistry*, 290, 8964–8974. <https://doi.org/10.1074/jbc.M114.616516>
- Radhakrishnan, V. M., Ramalingam, R., Larmonier, C. B., Thurston, R. D., Laubitz, D., Midura-Kiela, M. T., McFadden, R. M., Kuro-O, M., Kiela, P. R., & Ghishan, F. K. (2013). Post-translational loss of renal TRPV5 calcium channel expression, Ca(2+) wasting, and bone loss in experimental colitis. *Gastroenterology*, 145, 613–624. <https://doi.org/10.1053/j.gastro.2013.06.002>
- Rojas, E., Arispe, N., Haigler, H. T., Burns, A. L., & Pollard, H. B. (1992). Identification of annexins as calcium channels in biological membranes. *Bone and Mineral*, 17, 214–218. [https://doi.org/10.1016/0169-6009\(92\)90739-z](https://doi.org/10.1016/0169-6009(92)90739-z)
- Silvennoinen, J., Lamberg-Allardt, C., Kärkkäinen, M., Niemelä, S., & Lehtola, J. (1996). Dietary calcium intake and its relation to bone mineral density in patients with inflammatory bowel disease. *Journal of Internal Medicine*, 240, 285–292. <https://doi.org/10.1046/j.1365-2796.1996.25862000.x>
- Sokolow, S., Manto, M., Gailly, P., Molgó, J., Vandebrouck, C., Vanderwinden, J. M., Herchuelz, A., & Schurmans, S. (2004). Impaired neuromuscular transmission and skeletal muscle fiber necrosis in mice lacking Na/Ca exchanger 3. *The Journal of Clinical Investigation*, 113, 265–273. <https://doi.org/10.1172/JCI18688>
- Sosnoski, D. M., & Gay, C. V. (2008). NCX3 is a major functional isoform of the sodium-calcium exchanger in osteoblasts. *Journal of Cellular Biochemistry*, 103, 1101–1110. <https://doi.org/10.1002/jcb.21483>
- Stains, J. P., & Gay, C. V. (1998). Asymmetric distribution of functional sodium-calcium exchanger in primary osteoblasts. *Journal of Bone and Mineral Research: The Official Journal of the American Society for Bone and Mineral Research*, 13, 1862–1869. <https://doi.org/10.1359/jbmr.1998.13.12.1862>
- Stains, J. P., Weber, J. A., & Gay, C. V. (2002). Expression of Na(+)/Ca(2+) exchanger isoforms (NCX1 and NCX3) and plasma membrane Ca(2+) ATPase during osteoblast differentiation. *Journal of Cellular Biochemistry*, 84, 625–635.
- Tilg, H., Moschen, A. R., Kaser, A., Pines, A., & Dotan, I. (2008). Gut, inflammation and osteoporosis: Basic and clinical concepts. *Gut*, 57, 684–694. <https://doi.org/10.1136/gut.2006.117382>
- Wang, Z. X., Luo, Z. W., Li, F. X., Cao, J., Rao, S. S., Liu, Y. W., Wang, Y. Y., Zhu, G. Q., Gong, J. S., Zou, J. T., Wang, Q., Tan, Y. J., Zhang, Y., Hu, Y., Li, Y. Y., Yin, H., Wang, X. K., He, Z. H., Ren, L., ... Xie, H. (2022). Aged bone matrix-derived extracellular vesicles as a messenger for calcification paradox. *Nature Communications*, 13, 1453. <https://doi.org/10.1038/s41467-022-29191-x>
- Wei, Y., Tang, C., Zhang, J., Li, Z., Zhang, X., Miron, R. J., & Zhang, Y. (2019). Extracellular vesicles derived from the mid-to-late stage of osteoblast differentiation markedly enhance osteogenesis in vitro and in vivo. *Biochemical and Biophysical Research Communications*, 514, 252–258. <https://doi.org/10.1016/j.bbrc.2019.04.029>
- Wuthier, R. E., & Lipscomb, G. F. (2011). Matrix vesicles: structure, composition, formation and function in calcification. *Frontiers in Bioscience (Landmark edition)*, 16, 2812–2902. <https://doi.org/10.2741/3887>
- Xiao, Z., Camalier, C. E., Nagashima, K., Chan, K. C., Lucas, D. A., de la Cruz, M. J., Gignac, M., Lockett, S., Issaq, H. J., Veenstra, T. D., Conrads, T. P., & Beck, G. R. Jr (2007). Analysis of the extracellular matrix vesicle proteome in mineralizing osteoblasts. *Journal of Cellular Physiology*, 210, 325–335. <https://doi.org/10.1002/jcp.20826>

SUPPORTING INFORMATION

Additional supporting information can be found online in the Supporting Information section at the end of this article.

How to cite this article: Sheikh, I. A., Midura-Kiela, M. T., Herchuelz, A., Sokolow, S., Kiela, P. R., & Ghishan, F. K. (2024). The Na⁺/Ca²⁺ exchanger NCX3 mediates Ca²⁺ entry into matrix vesicles to facilitate initial steps of mineralization in osteoblasts. *Journal of Extracellular Vesicles*, 13, e12450. <https://doi.org/10.1002/jev2.12450>